Molecular Rotational Excitation by Strong Femtosecond Laser Pulses

Chengyin Wu,* Guiping Zeng, Hongyan Jiang, Yunan Gao, Nan Xu, and Qihuang Gong*

State Key Laboratory for Mesoscopic Physics and Department of Physics, Peking University, Beijing 100871, People's Republic of China

Received: June 18, 2009; Revised Manuscript Received: August 22, 2009

We study the rotational wave packet created by nonadiabatic rotational excitation of molecules with strong femtosecond laser pulses. The applicable condition of the Delta−Kick method is obtained by comparing the laser intensity and pulse duration dependences of the wave packet calculated with different methods. The wave packet evolution is traced analytically with the Delta−Kick method. The calculations demonstrate that the rotational populations can be controlled for the rotational wave packet created by two femtosecond laser pulses. The evolution of the rotational wave packet with controlled populations produces interference patterns with exotic spatial symmetries. These calculations are validated by comparing the theoretical calculations with our experimental measurements for the rotational wave packet created by thermal ensemble CO_2 and two strong femtosecond laser pulses. Potential applications in molecular science are also discussed for the rotational wave packet with controlled populations and spatial symmetries.

Introduction

Intense femtosecond laser pulses have become powerful tools to probe and control the behaviors of molecules.[1,2] A lot of exotic behaviors are observed for molecules in intense femtosecond laser fields depending on the laser intensity. When the laser intensity is below the ionization threshold, the interaction between the nonresonant laser field and the induced dipole moment of molecules tends to align the most polarizable molecular axis along the laser polarization direction.[3−5] There are two alternative ways to align molecules with strong laser fields depending on the pulse duration. When the pulse duration is longer than the molecular rotational period, the alignment vanishes after the laser is over. This alignment is called adiabatic alignment.[6,7] When the pulse duration is shorter than the molecular rotational period, the laser−molecule interaction gives the molecule a rapid kick to push the most polarizable molecular axis along the laser polarization direction and creates a coherent rotational wave packet.[8−10] The evolution of the rotational wave packet results in periodic transient alignment or antialignment after the laser is over. This alignment is called field-free alignment.[11−13] As compared with the adiabatic alignment, the advantage of the field-free alignment is that the aligned molecules can be obtained without the presence of an external electric field. The field-free-aligned molecules lead to a variety of new and exciting applications in many research fields.[14−17] Fleischer et al. experimentally accomplished isotope separation of $^{14}N_2$ and $^{15}N_2$ by this field-free alignment technique.[18] By measuring high harmonics generated from aligned molecules, Itatani et al. experimentally reconstructed the highest occupied molecular orbit of nitrogen.[19] During the past few years, two kinds of representative techniques have been developed experimentally to quantify the alignment degree of molecules. The first technique is to image the momentum of the ionic fragments by using another intense laser pulse to dissociate or explode the aligned molecules.[20−22] The alignment degree can be calculated from the angular distribution of the ionic fragments. The second technique is based on the birefringence caused by aligned molecules and can be called a noninvasive method. It uses another weak probe laser pulse to measure the birefringence induced by the transient aligned molecules. The depolarization of the probe laser represents the alignment degree of the molecules.[23−26] As compared with the former technique, the advantage of the latter one is that the probe laser is so weak that it does not destroy the aligned molecules, which is important for the measurement and application of an aligned molecular ensemble.

Controlling the molecular rotational wave packet using femtosecond laser pulse has attracted much attention in recent years.[27,28] Adaptive control and optimization of field-free molecular alignment was achieved both theoretically and experimentally by using phase- and amplitude-shaped femtosecond laser pulses.[29−32] It was reported that the coherent rotational wave packet and the molecular alignment can be further shaped by another strong femtosecond laser pulse or a train of laser pulses.[34−42] Selective alignment of molecular spin isomers was also achieved experimentally by using two nonresonant strong femtosecond laser pulses.[43,44] It was also shown that the wave packet revival can be switched on and off by modifying the phase between the rotational wave packet components with a relatively weak laser pulse at the fractional revivals.[45] In addition to one-dimensional field-free alignment, three-dimensional field-free molecular alignment is also being explored theoretically and experimentally.[46−48]

The component of rotational wave packet is crucial to many molecular processes, such as strong field dissociation and chemical reaction dynamics. In a recent communication,[49] we proposed a control scheme for selecting populations of molecular rotational states by wave packet interference. The evolution of the rotational wave packet with selected populations produces some interference patterns with exotic spatial symmetries. In this paper, we present a full account of this work. The applicable condition of the Delta−Kick method is obtained by comparing the theoretical results calculated with different methods. The quantum-state distributions and angular distributions are also calculated for the rotational wave packet created by one or two

* To whom correspondence should be addressed. E-mail: cywu@pku.edu.cn (C.W.) or qhgong@pku.edu.cn (Q.G.).

10.1021/jp905743v CCC: $40.75
Published on Web 09/11/2009

strong femtosecond laser pulses. The results demonstrate that a molecular ensemble with selected quantum-state distributions and controlled spatial distributions can be obtained under field-free conditions.

Theory

1. Creation of a Rotational Wave Packet. A rotational wave packet is created by nonadiabatic rotational excitation of molecules with strong femtosecond laser pulses. Because the pulse duration is much shorter than the molecular rotational period, the coherence of the wave packet is preserved after the laser is over. The evolution of the rotational wave packet results in the transient alignment or antialignment without the presence of an external field. In this section, we utilize two methods to calculate the wave packet created by one strong femtosecond laser pulse. One commonly used is the Crank−Nicholson method, and the other is the Delta−Kick method. Through comparing the results calculated by these two methods, the applicable condition is obtained for the Delta−Kick method.

For a linear molecule irradiated by a nonresonant linearly polarized laser field, the laser−molecule interaction can be expressed by:

$$U(t) = -\frac{1}{4}E_0^2 f^2(t)(\Delta\alpha \cos^2\theta) \quad (1)$$

where θ is the polar angle between the molecular axis and the laser polarization direction, E_0 and $f(t)$ are the amplitude and envelope of the laser electric field respectively, and $\Delta\alpha$ is the molecular polarizability anisotropy.

For the Crank−Nicholson method, the time-dependent Schrödinger equation $i\hbar(\partial)/(\partial t)\Psi(t) = H\Psi(t)$ can be numerically solved by the split-operator technique and written as:[50]

$$[1 + i\Delta t H(t + \Delta t)/2\hbar]\Psi(t + \Delta t) = [1 - i\Delta t H(t)/2\hbar]\Psi(t) \quad (2)$$

where $H(t) = BJ^2 + U(t)$ with BJ^2 being the rotational energy operator. In the angular momentum representation, the wave function for the wave packet at the end of the laser pulse can be expressed as:

$$\Psi = \sum_{J\geq|M_0|} A_{J,M_0}|J, M_0\rangle \quad (3)$$

where $|J, M_0\rangle$ are the spherical harmonic functions and A_{J,M_0} are their coefficients. $|A_{J,M_0}|^2$ determines the population at the rotational states $|J, M_0\rangle$ in the wave packet. Similarly, if a second laser pulse is introduced after a time delay, the above procedure is repeated, and the wave packet is obtained after the second laser pulse.

For the Delta−Kick method, because the laser duration τ is much shorter than the molecular rotational period T_r, the laser−molecule interaction can be approximated as a δ potential and can be written as:

$$U(\theta, \lambda) = -\lambda \cos^2\theta\, \delta(t) \quad (4)$$

with $\lambda = (1/4)\cdot\Delta\alpha\cdot E_0^2\cdot\int_0^{2\tau} f^2(t)\, dt$.[51] Suppose that the molecular ensemble is initially populated at the rotational state $|J_0, M_0\rangle$ and is excited by a strong femtosecond laser pulse. The laser-induced nonadiabatic rotational excitation results in a rotational wave packet composed of a serial of rotational states while preserving the azimuthal quantum number as the initial value M_0. After the laser is over, the rotational wave packet can be described by eq 3 with

$$A_{J,M_0} = \langle J, M_0|\exp(i\lambda \cos^2\theta/\hbar)|J_0, M_0\rangle \quad (5)$$

Its value can be calculated by the following numerical integration

$$A_{J,M_0} = \int_0^{2\pi} d\varphi \int_0^{\pi} \sin\theta\, d\theta\, Y^*_{J,M_0}\exp(i\lambda \cos^2\theta/\hbar)Y_{J_0,M_0} \equiv C_{J,J_0}(\lambda, M_0) \quad (6)$$

where $Y^*_{J,M_0}(\theta,\varphi)$ is the complex conjugate of the spherical harmonic function $Y_{J,M_0}(\theta,\varphi)$. It can be seen that $C_{J,J_0}(\lambda,M_0)$ is determined by the laser pulse parameters. The above Delta−Kick approximation greatly simplifies the theoretical calculation, especially for the multipulse calculation. For example, at the end of the second laser pulse, the wave packet created by two identical pulses with a delay time of Δt can be given by

$$\Psi = \sum_{J\geq|M_0|}\sum_{J_i\geq|M_0|} C_{J_i,J_0}(\lambda, M_0)\cdot e^{-iE_{J_i}\Delta t/\hbar}\cdot C_{J,J_i}(\lambda, M_0)|J, M_0\rangle \quad (7)$$

where $E_{J_i} = B_0 J_i(J_i + 1)$ is the energy for rotational state and B_0 is the rotational constant. The intermediate states J_i are populated by the first laser pulse.

2. Characterization of a Rotational Wave Packet. The evolution of the rotational wave packet is usually characterized by the time-dependent alignment parameter $\langle\cos^2\theta\rangle(t) = \langle\Psi(t)|\cos^2\theta|\Psi(t)\rangle$, which is given by:[24]

$$\langle\cos^2\theta\rangle(t)_{J_0,M_0} = \sum_J \{|A_{J,M_0}|^2 c_{J,J} + 2|A_{J,M_0}||A_{J+2,M_0}| \times \cos[\Delta\varphi_{J,J+2}(t)]c_{J,J+2}\} \quad (8)$$

with

$$\begin{aligned} c_{J,J} &= \langle J, M_0|\cos^2\theta|J, M_0\rangle \\ c_{J,J+2} &= \langle J, M_0|\cos^2\theta|J + 2, M_0\rangle \\ \Delta\varphi_{J,J+2}(t) &= \omega_{J+2,J}t + \Delta\varphi_{J,J+2}(0) \end{aligned} \quad (9)$$

where $\omega_{J+2,J} = (E_{J+2} - E_J)/\hbar$ are the beat frequencies between the states $|J + 2, M_0\rangle$ and $|J, M_0\rangle$, and $\Delta\varphi_{J,J+2}(0)$ is the phase difference at the end of the laser pulse.[22]

From the expression of $\langle\cos^2\theta\rangle$ above, we can see that the phase difference $\Delta\varphi_{J,J+2}(t)$ determines the value of the alignment parameter $\langle\cos^2\theta\rangle$. When $\Delta\varphi_{J,J+2}(t) \rightarrow 0$ or 2π, $\langle\cos^2\theta\rangle$ approaches maximum, in which the molecule is predominantly aligned along the laser polarization and labeled as aligned molecule. When $\Delta\varphi_{J,J+2}(t) \rightarrow \pi$, $\langle\cos^2\theta\rangle$ approaches minimum, in which the molecule is concentrated in a plane orthogonal to the laser polarization and labeled as an antialigned molecule. Although the time-dependent alignment parameter $\langle\cos^2\theta\rangle$ provides a good characterization for the evolution of the rotational wave packet, it also wipes off a lot of information of the molecular rotational wave packet in the process of quantum

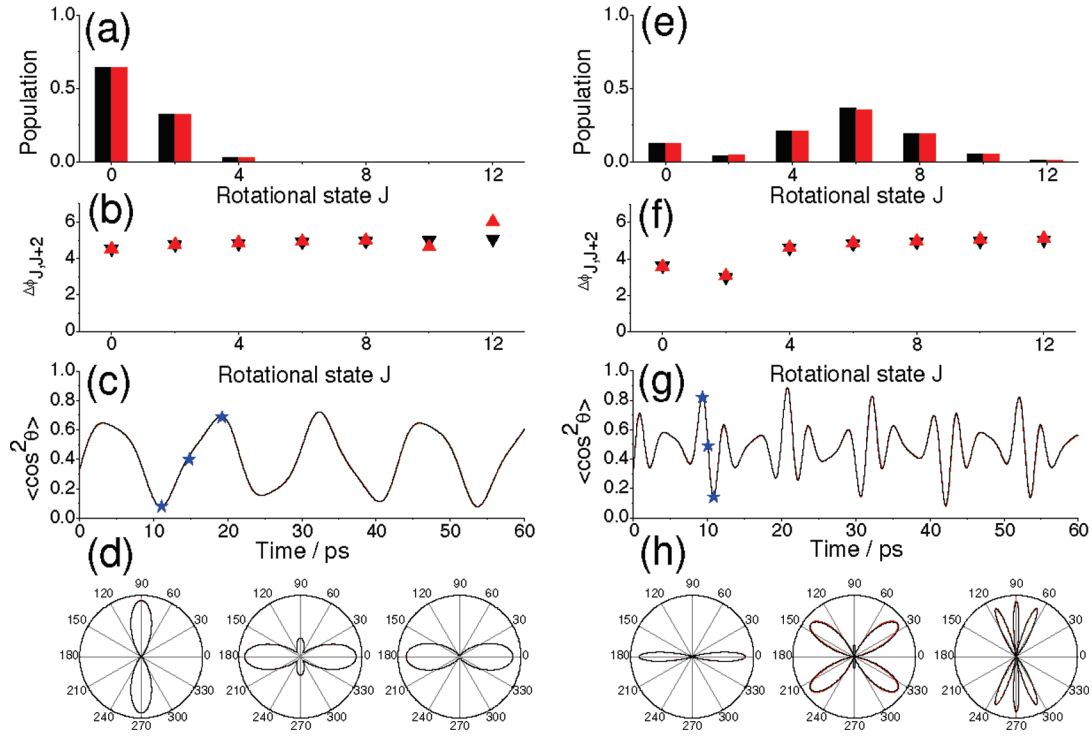

Figure 1. (a) Population and (b) phase differences at the end of the pulse and (c) time-dependent alignment parameter $\langle\cos^2\theta\rangle$ and (d) angular distributions at different times (marked with asterisk in panel c) for the wave packet of CO_2 created by one 110 fs, 800 nm laser pulse at an intensity of 5.0×10^{12} W/cm^2. (e) Population and (f) phase differences at the end of the pulse and (g) time-dependent alignment parameter $\langle\cos^2\theta\rangle$ and (h) angular distributions at different times (marked with asterisk in panel g) for the wave packet of CO_2 created by one 110 fs, 800 nm laser pulse at an intensity of 2.0×10^{13} W/cm^2. Black and red data denote the results calculated with the Crank−Nicholson method and the Delta−Kick method, respectively. The initial ensemble of CO_2 molecules is populated at the ground rotational state $J_0 = 0$ and $M_0 = 0$ before laser irradiation.

average. To acquire more information about the rotational wave packet, we have calculated the angular distribution of the molecular ensemble as the squared modulus of the rotational wave function:[52]

$$\rho(\theta,\varphi,t) = |\Psi|^2 = \sum_{J\geq|M_0|}\sum_{J'\geq|M_0|} A_{J,M_0}(t)A^*_{J',M_0}(t)Y_{J,M_0}(\theta,\varphi)Y^*_{J',M_0}(\theta,\varphi) \quad (10)$$

where $A_{J,M_0}(t)$ is the coefficient of the states $|J, M_0\rangle$ at time t. Note that although the expression above has two azimuth angles, actually the angular distribution of the wave packets is independent of azimuth angle φ. So, we will give the angular distribution of the wave packet only on azimuth angle θ in this article.

Experimental Method

The experimental method has been described in our previous paper.[53] An 800 nm, 110 fs laser pulse is divided into two parts to provide a strong energy pump beam and a weak energy probe beam. The pump beam is linearly polarized, and the probe beam is slightly elliptically polarized. Both the pump beam and the probe beam are focused with a 30 cm focal length lens into a 20 cm long gas cell at a small angle. The pure heterodyne alignment signal is obtained by subtracting the two heterodyne signals measured respectively by a left-handed and right-handed elliptically polarized probe laser. These data directly reproduce the revival structure of the wave packet, and its Fourier transform spectrum provides the information about the rotational population in the wave packet. For demonstrating our control scheme about the rotational wave packet, the strong pump beam is divided into another two parts. One is for aligning the molecules, and the other is for controlling the population. Their relative time delays among these laser beams can be precisely adjusted by two computer-controlled optical translational stages.

Results and Discussion

This section will be divided into three parts. First, we calculate the wave packet of CO_2 created by one 110 fs laser pulse using both the Crank−Nicholson method and the Delta−Kick method. In the calculation, the initial CO_2 is supposed to be populated at the ground rotational state $J_0 = 0$ and $M_0 = 0$. On the basis of these calculations, we obtain the applicable condition of the Delta−Kick method for CO_2. Next, we calculate the wave packet of CO_2 created by two 110 fs laser pulses at arbitrary time delays. The results demonstrate that a molecular ensemble with selected quantum-state distributions and controlled spatial distributions can be obtained under field-free condition with two strong femtosecond laser pulses. Finally, the above theoretical calculations are validated by comparing the theoretical prediction with our experimental measurement for the rotational wave packet created by thermal ensemble CO_2 and two strong femtosecond laser pulses.

1. Rotational Wave Packet Created by One Laser Pulse. Figure 1a shows the rotational populations for the rotational wave packet of CO_2 irradiated by one 800 nm, 110 fs laser pulse at an intensity of 5×10^{12} W/cm^2. Nonadiabatic rotational excitation of molecules results in a rotational wave packet consisting of $J = 0-6$, while most of the molecules still remain at the initial ground state. Figure 1b shows the phase differences $\Delta\varphi_{J,J+2}(0)$ at the end of the laser pulse. It can be seen that the

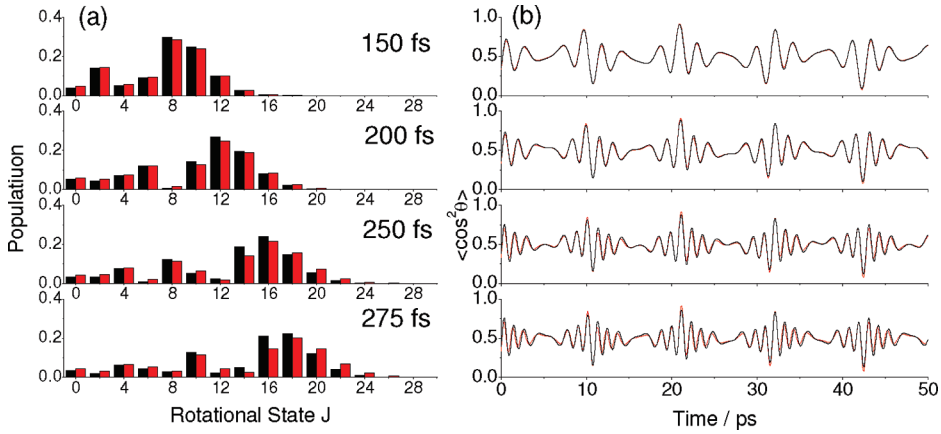

Figure 2. (a) Population and (b) time-dependent alignment parameter $\langle\cos^2\theta\rangle$ calculated using the Crank−Nicholson method (in black) and the Delta−Kick method (in red) for the rotational wave packet created by a strong laser pulse with different pulse durations. The laser intensity is 2.0×10^{13} W/cm^2. The initial ensemble of CO_2 molecules is populated at the ground rotational state $J_0 = 0$ and $M_0 = 0$ before laser irradiation.

phase differences between two adjacent rotational states are near constant at the end of the laser pulse and a coherent rotational wave packet is formed. Figure 1c shows the time-dependent alignment parameter $\langle\cos^2\theta\rangle$ for the rotational wave packet, which varies between 0 and 1. The evolution of the alignment parameter is slow because only few rotational states are populated. Figure 1d depicts the angular distributions of the wave packet at 11.09, 15.14, and 19.21 ps, respectively. The time-dependent angular distribution reflects the evolution of the wave packet elaborately. At the maximum of the alignment parameter $\langle\cos^2\theta\rangle$, the molecular axis mainly distributes around the laser polarization direction, while at the minimum of the alignment parameter $\langle\cos^2\theta\rangle$, the molecular axis mainly distributes around a plane orthogonal to the laser polarization direction. To study the effect of laser intensity on the rotational wave packet, we increase the laser intensity to 2.0×10^{13} W/cm^2. At this laser intensity, the wave packet created by nonadiabatic rotational excitation populates up to $J = 12$, with a peak population at $J = 6$, as shown in Figure 1e. Figure 1f shows the phase differences $\Delta\varphi_{J,J+2}(0)$ at the end of laser pulse, where the phase differences between adjacent rotational states are almost constant. These calculations are consistent with previous reports.[32] Figure 1g shows the time-dependent alignment parameter $\langle\cos^2\theta\rangle$. As compared with Figure 1c, the alignment parameter evolves much faster because more rotational states are populated. We also calculate the angular distribution at three different times from the maximum to the minimum of the alignment parameter. The times are 9.31, 10.05, and 10.80 ps, respectively. The results are depicted in Figure 1h. To compare the effectiveness of the Delta−Kick method, we have depicted the results of the Crank−Nicholson method and the Delta−Kick method in black and red lines, respectively, in Figure 1. The agreements between these two theoretical methods are satisfactory for pulse duration of 110 fs.

However, the effectiveness of the Delta−Kick method will reduce as the pulse duration increases. To obtain the application condition of the Delta−Kick method, we compare the results of the rotational wave packet calculated by the Crank−Nicholson method and the Delta−Kick method with different pulse durations. The laser intensity is 2.0×10^{13} W/cm^2. The pulse duration varies from 150 to 275 fs. The population and alignment parameter $\langle\cos^2\theta\rangle$ of the rotational wave packet are shown in Figure 2a,b, respectively. The plots in black and red lines denote the results of the Crank−Nicholson method and the Delta−Kick method, respectively. It can be seen that the differences between these two theoretical methods become large with increasing pulse durations, especially for the rotational populations. When the pulse duration is shorter than 200 fs, the agreement between the two methods is still satisfying. However, when the pulse duration is longer than 250 fs, the differences between these two methods become obvious. These results demonstrate that we can use the Delta−Kick method to trace the rotational wave packet of CO_2 created by strong femtosecond laser pulse with a pulse duration shorter than 200 fs.

2. Rotational Wave Packet Created by Two Laser Pulses. The Delta−Kick method introduced in the previous section makes it feasible to analytically trace the evolution of the wave packet created by strong femtosecond laser pulses. The molecular ensemble initially locates at the rotational state $|J_0, M_0\rangle$ before the laser excitation. After being excited by a strong femtosecond laser pulse, the molecule is excited to different rotational states. A wave packet is therefore created and is shown in eq 3. After the laser is over, the wave packet evolves as follows:

$$\Psi^{(1)} = \sum_{J_i^1 \geq M_0} A_{J_i^1} e^{-iE_{J_i^1}t/\hbar} |J_i^1, M_0\rangle \tag{11}$$

At a time delay Δt, the second strong femtosecond laser pulse is introduced to manipulate the rotational wave packet. When the second laser pulse is over, each eigenstate $|J_i^1, M_0\rangle$ is excited to another serial of rotational states and form another rotational wave packet $\sum_{J_k^2 \geq |M_0|} A_{J_i^1} e^{-iE_{J_i^1}\Delta t/\hbar} \cdot C_{J_k^2,J_i^1}(\lambda, M_0)|J_k^2, M_0\rangle$ where $C_{J_k^2,J_i^1}(\lambda, M_0)$ have been defined in eq 6. Quantum superposition among these rotational wave packets produces the final rotational wave packet, whose evolution can be written as:

$$\Psi^{(2)} = \sum_{J_k^2 \geq M_0} A_{J_k^2} \cdot e^{-iE_{J_k^2}(t-\Delta t)/\hbar} |J_k^2, M_0\rangle \tag{12}$$

with

$$A_{J_k^2} = \sum_{J_i^1 \geq |M_0|} A_{J_i^1} \cdot e^{-iE_{J_i^1}\Delta t/\hbar} \cdot C_{J_k^2,J_i^1}(\lambda, M_0) \tag{13}$$

The population of the rotational state J_k^2 is determined by the square of the amplitude of $A_{J_k^2}$. It consists of the contributions from different intermediate rotational states J_i^1, which are

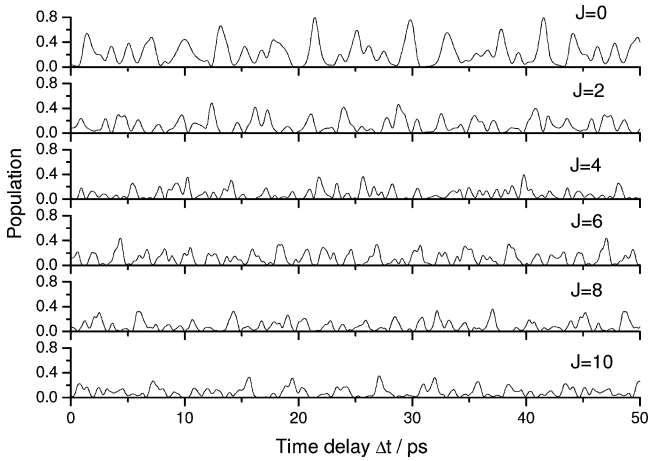

Figure 3. Population of each rotational eigenstate as a function of the time delay between the two laser pulses. The laser has a central wavelength of 800 nm, a pulse duration of 110 fs, and an intensity of 2.0×10^{13} W/cm^2. The initial ensemble of CO_2 molecules is populated at the ground rotational state $J_0 = 0$ and $M_0 = 0$ before laser irradiation.

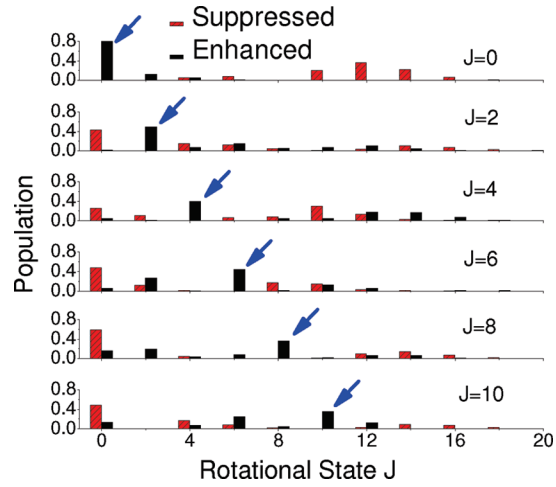

Figure 4. Population for the rotational wave packet with a specific rotational eigenstate being suppressed (in red) or enhanced (in black). The laser has a central wavelength of 800 nm, a pulse duration of 110 fs, and an intensity of 2.0×10^{13} W/cm^2. The initial ensemble of CO_2 molecules is populated at the ground rotational state $J_0 = 0$ and $M_0 = 0$ before laser irradiation.

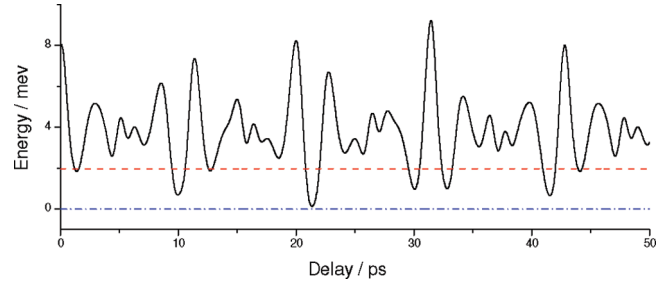

Figure 5. Average rotational energy for the rotational wave packet formed by two 800 nm, 110 fs, 2.0×10^{13} W/cm^2 laser pulses as a function of the delay time between the two laser pulses. The average rotational energy is 0 meV before laser excitation (blue dash dot line) and 1.97 meV after one 800 nm, 110 fs, 2.0×10^{13} W/cm^2 laser pulse excitation (red dash line). The initial ensemble of CO_2 molecules is populated at the ground rotational state $J_0 = 0$ and $M_0 = 0$ before laser irradiation.

populated by the first laser pulse. Depending on the time delay Δt between the two laser pulses, these contributions are constructive or destructive interference. The former enables the population to be enhanced and the latter to be suppressed for a specific rotational state in the final wave packet created by the two laser pulses.

Figure 3 shows the population for each specific rotational state in the wave packet as a function of the time delay between the two laser pulses. The laser pulse has a central wavelength of 800 nm, a pulse duration of 110 fs, and an intensity of 2.0×10^{13} W/cm^2. The CO_2 molecular ensemble is prepared initially at the ground rotational state $J_0 = 0$ and $M_0 = 0$ before the laser excitation. The results demonstrate that the rotational population strongly depends on the time delay between the two laser pulses. The oscillatory dependence of the rotational population on the time delay is observed by Meijer et al. for NO irradiated by two femtosecond laser pulses.[54] The population for a specific rotational state has a large dynamic range in the rotational wave packet created by two laser pulses. For example, the population at $J = 2$ is 5.0% in the rotational wave packet created by one laser pulse as shown in Figure 1e. However, for the rotational wave packet created by two laser pulses, the population at $J = 2$ can be varied between 48.6% (time delay is 12.36 ps) and 0.0% depending on the time delay between the two laser pulses. The maximum and minimum population for a specific eigenstate can be further optimized by adjusting other parameters of the two laser pulses, such as laser intensity and pulse duration. Therefore, double pulse technique provides a feasible approach to control the populations of the rotational wave packet.

Figure 4 shows the populations of the rotational wave packet created by two 110 fs, 800 nm laser pulses at an intensity of 2.0×10^{13} W/cm^2. The population can be effectively suppressed or enhanced for a specific rotational state by adjusting the time delay between the two laser pulses. The minimum population can reach zero for each rotational state. The maximum population is greatly improved for a specific rotational state in the wave packet created by two laser pulses relative to that in the wave packet created by one laser pulse. The maximum and minimum population is easily achieved for the rotational wave packet created by two laser pulses by precisely adjusting the time delay between two laser pulses. This kind of molecular system is very helpful to carry out the study of state-to-state chemical reaction dynamics. The above results demonstrate that the population can be actively controlled for a specific rotational state in the rotational wave packet created by two strong femtosecond laser pulses. Therefore, the rotational wave packet has different energies depending on the time delay between the two laser pulses.

Figure 5 shows the calculated average rotational energy for the rotational wave packet formed by the two strong femtosecond laser pulses. The average rotational energy is 0 meV before laser irradiation and is shown by the blue dash dot line. The energy is increased to 1.97 meV after one 800 nm, 110 fs, 2.0×10^{13} W/cm^2 laser pulse irradiation and is shown by the red dash line. The black solid line gives the average rotational energies after irradiation with two 800 nm, 110 fs, 2.0×10^{13} W/cm^2 laser pulses as a function of delay time between the two laser pulses. It can be seen that the second laser pulse increases or decreases the rotational energy of the rotational wave packet created by the first laser pulse, depending on the time delay between the two laser pulses. When the delay time is 21.34 ps, the final rotational wave packet has the lowest rotational energy of 0.13 meV. This energy is much lower than the rotational energy of the wave packet created by the first laser pulse but higher than the rotational energy of the molecule before the

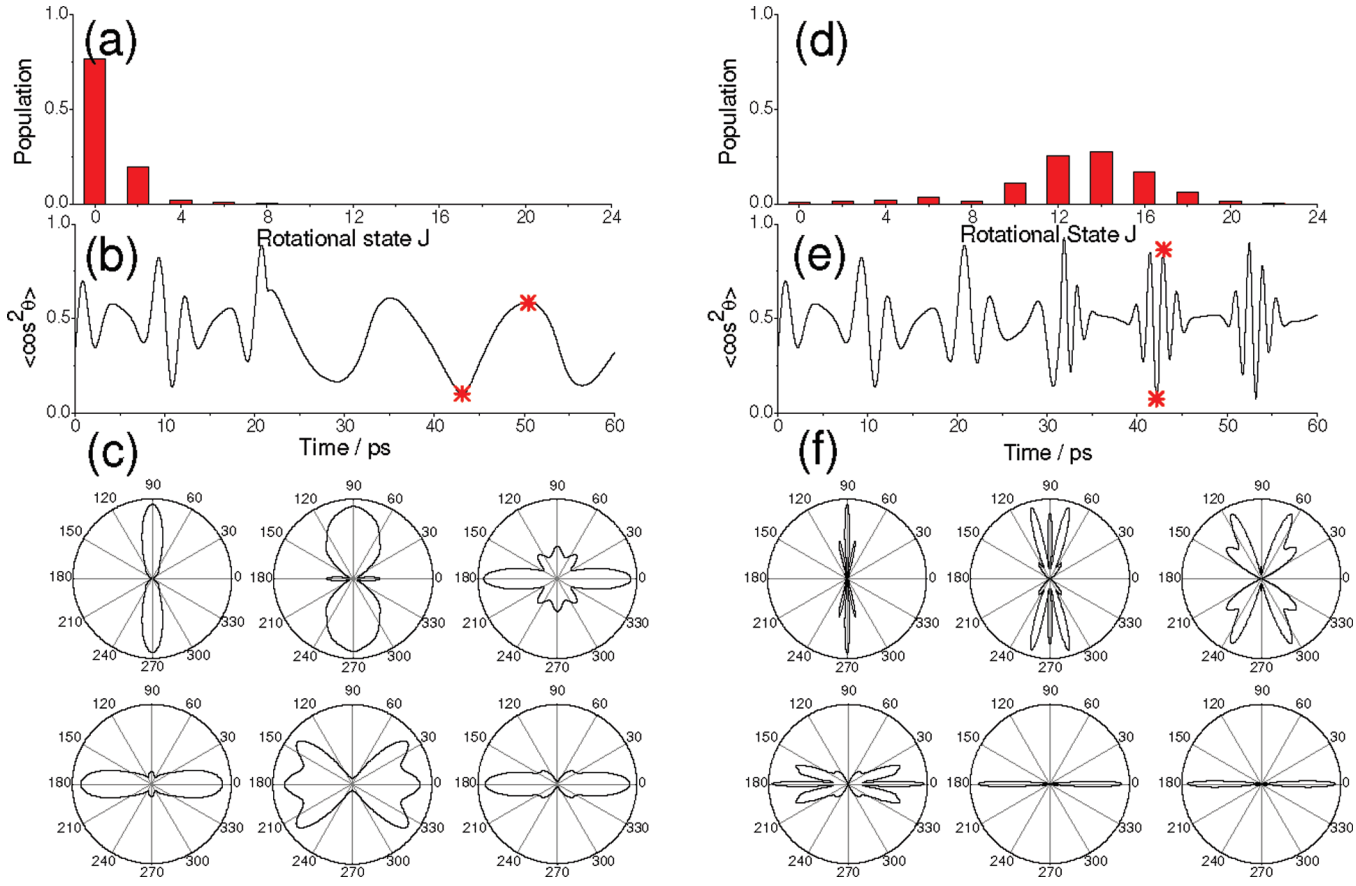

Figure 6. (a) Population and (b) time-dependent alignment parameter $\langle\cos^2\theta\rangle$ and (c) angular distributions at different times between 43.76 and 51.17 ps (marked with asterisk in panel b) for the rotational wave packet created by two strong femtosecond laser pulses with a delay time of 21.34 ps. (d) Population and (e) time-dependent alignment parameter $\langle\cos^2\theta\rangle$ and (f) angular distributions at different times between 42.17 and 42.90 ps (marked with asterisk in panel e) for the rotational wave packet created by two strong femtosecond laser pulses with a delay time of 31.44 ps. The initial ensemble of CO_2 molecules is populated at the ground rotational state $J_0 = 0$ and $M_0 = 0$ before laser irradiation.

laser excitation. This result demonstrates that the wave packet created by the first laser pulse cannot return to the original one $|J_0 = 0, M_0 = 0\rangle$ by the second laser pulse. In other words, perfect annihilation cannot be obtained by a pulse pair, which is consistent with previous reports.[32,39] When the delay time is 31.44 ps, the final rotational wave packet has the highest rotational energy of 9.20 meV.

Figure 6a shows the populations of the rotational wave packet created by two strong femtosecond laser pulses with a delay time of 21.34 ps. At this time delay, the final rotational wave packet has the lowest rotational energy and the rotational states mainly distribute in $J = 0$ and 2. Figure 6b shows the alignment parameter $\langle\cos^2\theta\rangle$ as a function of time. It changes more slowly than that of the rotational wave packet created by a single femtosecond laser pulse. To provide a more complete description of the final rotational wave packet, we have calculated the time-dependent angular distribution of the rotational wave packet. Figure 6c shows the angular distributions at the time of 43.76, 45.08, 46.40, 48.38, 49.70, and 51.17 ps, respectively. The rotational wave packet displays a rich variety of spatial symmetries between the aligned and the antialigned distributions. Figure 6d shows the populations of the rotational wave packet created by two strong femtosecond laser pulses with a time delay of 31.44 ps. At this time delay, the final rotational wave packet has the highest rotational energy, and the rotational states distribute among $J = 0-22$ with a peak population at $J = 14$. Figure 6e shows the time-dependent alignment parameter $\langle\cos^2\theta\rangle$. It changes faster than that of the rotational wave packet with the lowest rotational energy because more rotational states are populated. Figure 6f shows the angular distributions of the rotational wave packet at the time of 42.17, 42.31, 42.44, 42.63, 42.77, and 42.90 ps, respectively. The angular distribution changes much faster and displays exotic spatial symmetries. With these time-dependent angular distributions for rotational wave packet with selected populations, the rotational quantum state might be reconstructed experimentally.[55] These calculations show that the alignment degree and the evolution speed can be manipulated for the rotational wave packet created by two laser pulses by adjusting the time delay.

3. Comparison between Experimental Measurements and Theoretical Calculations. The above theoretical calculations for rotational excitation can be tested with the current experimental technologies. The initial single rotational state can be realized by supersonic cooling or selected by a hexapole electric field.[33,56] The populations in the wave packet can be decoded by state-resolved resonant-enhanced multiphoton ionization,[57] and the time-dependent angular distributions can be mapped by Coulomb explosions.[15] Unfortunately, these complicated apparatus are not available in our laboratory. Here, we verify the above theoretical calculations by comparing the calculated alignment parameter $\langle\cos^2\theta\rangle$and the experimental measured values for thermal assemble CO_2 by two strong femtosecond laser pulses. For the thermal assemble with a rotational temperature T, we calculate the rotational wave packet dynamics $\langle\cos^2\theta\rangle(t)_{J,M}$ for each initial rotational state $|J, M\rangle$. The alignment parameter is obtained by incoherently averaging the $\langle\cos^2\theta\rangle(t)_{J,M}$ over all initial rotational states $|J, M\rangle$ weighted by the Boltzmann distribution:

$$\langle\cos^2\theta\rangle(t) = \frac{\sum_{J,M} g_J \exp(-E_J/kT)\langle\cos^2\theta\rangle(t)_{J,M}}{\sum_J g_J(2J+1)\exp(-E_J/kT)} \quad (14)$$

where g_J is the nuclear spin statistics factor of a homonuclear diatomic molecule. Although CO_2 is not actually a homonuclear diatomic molecule, the two O atoms are indistinguishable. The symmetrization of the wave function with respect to these two O atoms requires $g_J = 0$ for odd rational states and $g_J = 1$ for even rational states.

In the current experimental measurement, three precisely timed laser pulses are used. The first strong laser pulse creates a coherent rotational wave packet from an initial thermal ensemble of CO_2 at room temperature. The second strong laser pulse shapes the rotational wave packet and controls its population. The third weak laser pulse probes the time evolution of the rotational wave packet by using the pure heterodyne weak laser polarization technique.[53] The black line in Figure 7a is the experimental measured alignment signals of thermal assemble CO_2 by a laser pulse with a central wavelength of 800 nm and pulse duration of 110 fs. The advantage of the pure heterodyne weak laser polarization technique is that the signal directly reproduces the alignment parameter $\langle\cos^2\theta\rangle$ without destroying the aligned molecules. The pulse energy is 200 μJ, and the laser intensity is estimated to be 1.0×10^{13} W/cm^2 based on the laser focus measurement using a standard knife edge method. The alignment signal is proportional to $[\langle\cos^2\theta\rangle - (1/3)]$ and directly reproduces the evolution of the alignment parameter $\langle\cos^2\theta\rangle$. The red dashed line shows the results of theoretical calculations by the Delta−Kick method. When the laser intensity in the simulations is taken to be 7.3×10^{12} W/cm^2, there is the best agreement between the theoretical calculation and the experimental measurement. Because we did not consider the volume effect and the spatial overlap between the aligning pulse and the probe pulse, the difference of the laser intensity between the experiment and the theory is within a reasonable range. Figure 7b shows the pure heterodyne alignment signal of CO_2 excited by two laser pulses separated by $\Delta t = 21.01$ ps. The energy of the second pulses is 80 μJ. The alignment parameter of the wave packet created by the first laser pulse is obviously enhanced even though the energy of the second laser pulse is much lower than that of the first laser pulse. Figure 7c shows the pure heterodyne alignment signal of CO_2 excited by two laser pulses separated by $\Delta t = 21.36$ ps. The energy of the second laser pulse is 160 μJ. The wave packet created by the first laser pulse is approximately annihilated by the second laser pulse. Here, it should be noticed that the intensity of the two laser pulses in theoretical simulations is the same with 7.3×10^{12} W/cm^2. This is because in the experiment, the wave packet created by the first laser pulse will relax to the lower rotational states in the process of evolution when the second laser pulse is applied. To experimentally annihilate the wave packet perfectly, the intensity of the second laser pulse is a little lower than that of the first laser pulse. For the above two cases, the second laser pulse is applied around the first quarter revival, where all of the components evolve in phase for the rotational wave packet created by the first laser pulse. The second laser has the same effects on all components of the wave packet. The molecule is excited to higher rotational states or returns back to the initial thermal distribution. As a result, the wave packet created by the first laser pulse is enhanced ($\Delta t = 21.01$ ps) or annihilated ($\Delta t = 21.36$ ps) by the second laser pulse. Figure 7d shows the pure heterodyne alignment signal of CO_2 excited by two laser pulses separated by $\Delta t = 12.98$ ps. Each pulse has an energy of 200 μJ. Different from the revival structures shown in Figure 7b,c, there are three series of revival structures in Figure 7d. The first series of revival structures located at $t = n\cdot(T_r/4)$ are created by the first laser pulse, and n is an integer number. The second series of revival structures located at $n\cdot(T_r/4) + \Delta t$ are created by the second laser pulse. The third series of revival structures located at $n\cdot(T_r/4) + 2\Delta t$ are created by the two laser pulses. These results show that the rotational wave packet created by the first laser pulse is split into two wave packets after the excitation of the second laser pulse. Their revival structures respectively locate at $t = n\cdot(T_r/4)$ and $n\cdot(T_r/4) + 2\Delta t$. The different revival structures for the rotational wave packet created by two laser pulses with different time delays originate from different components that evolve with different frequencies. The phases are different for the components of the rotational wave packet created by the first laser pulse when the second laser pulse is applied at $\Delta t = 12.98$ ps. Some rotational states are populated, and others are depopulated. The split of the wave packet predicted by the theoretical calculation is consistent with the experimental measurement. The satisfying agreements between the experimental measurements and the theoretical calculations validate our aforementioned control scheme of rotational wave packet. Both the quantum-state and the spatial distributions can be controlled under field-free conditions for the rotational wave packet created by two strong femtosecond laser pulses.

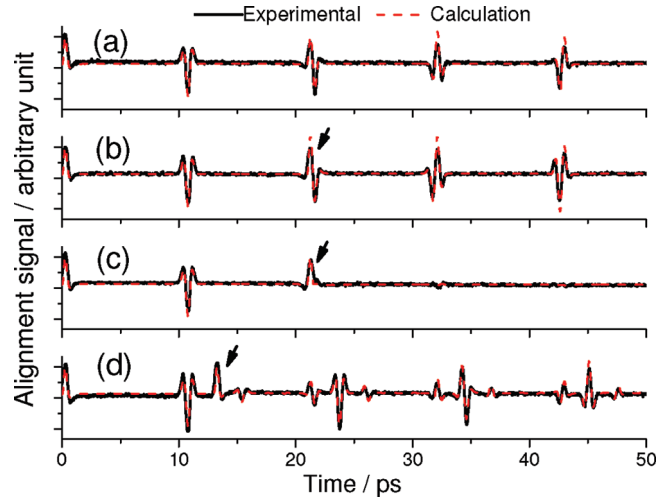

Figure 7. Pure heterodyne alignment signal for CO_2 at room temperature irradiated by (a) one laser pulse, (b) two laser pulses separated by $\Delta t = 21.01$ ps, (c) two laser pulses separated by $\Delta t = 21.36$ ps, and (d) two laser pulses separated by $\Delta t = 12.98$ ps. The arrow represents the moment that the second laser pulse is applied.

4. Discussion: Applications of Rotational Wave Packet with Selected Populations and Controlled Spatial Symmetries. One of the goals in molecular dynamics is to elucidate and control chemical reactions at the molecular level. This requires the simultaneous control of molecular three-dimensional spatial orientation and the internal quantum state distribution of the reactant. To achieve this goal, the initial single rotational state prepared by supersonic cooling or a hexapole electric field is usually oriented by the dc electric field.[56,58,59] However, the strong dc electric field technique is not a general approach. It is only suitable for molecules that have a large permanent dipole moment. In addition, the existence of the electric field will hinder the subsequent measurement. For example, the electron angular distribution produced by multiphoton ionization of oriented molecules will be distorted by the large dc electric field.

Femtosecond lasers have become powerful tools to align molecules. Through interacting with anisotropic polarizability of a molecule, the most polarizable axis of the molecule will be torqued into the laser polarization direction, and a rotational wave packet will be created. Because the pulse duration of femtosecond laser is much shorter than the molecular rotational period, the evolution of the rotational wave packet results in the transient alignment without the presence of the electric field. Three-dimensional field-free alignment of molecules is also recently experimentally demonstrated by using two femtosecond laser pulses with crossed polarizations.[46,47] The femtosecond laser-induced field-free alignment of molecules has the following advantages as compared with the above static electric field technique. First, it is a general approach. It can be applied to any molecule with anisotropic polarizabilities, whether the molecule has a permanent dipole moment or not. Second, it produces field-free-aligned molecules for applications to molecular dynamics studies. It is important that the aligned molecules are obtained without the presence of strong external electric fields as such fields would influence the behavior of the molecules.

However, the above field-free-aligned molecules induced by one strong laser pulse have obvious disadvantages. The rotational wave packet created by one femtosecond laser is composed of a serial of rotational states even though their populations depend on laser parameters, such as laser intensity and pulse duration. In our present control scheme, the population can be enhanced or suppressed for a specific rotational state by the constructive or destructive interference among these wave packets created by two strong femtosecond laser pulses. The evolution of the rotational wave packet with selected populations produces controlled interference patterns with exotic spatial symmetries. Therefore, rotational wave packet with selected populations opens a new way to prepare an initial reactant with controlled quantum-state populations and spatial distributions. This kind of molecular system is helpful in elucidating molecular dynamics at the molecular level.

Conclusions

We have theoretically calculated the rotational wave packet created by a strong femtosecond laser pulse using both the Crank−Nicholson method and the Delta−Kick method. Through comparing the populations, the alignment parameter and the time-dependent angular distribution of the rotational wave packet created by one strong laser pulse with different intensities and pulse durations, we obtain the applicable condition of the Delta−Kick method. Using the Delta−Kick method to trace the evolution of wave packet, we demonstrate that the rotational population can be enhanced or suppressed for a specific rotational state in the wave packet created by two strong femtosecond laser pulses through adjustment of the delay time between the two laser pulses. Further calculations show that the evolution of the rotational wave packet with selected populations produces controlled interference patterns with exotic spatial symmetries. The above calculations are verified by comparing the theoretical calculations with our experimental measurements for the rotational wave packet created by thermal ensemble CO_2 and two strong femtosecond laser pulses with arbitrary delay times. These results demonstrate that the double-pulse method enables the spatial distribution and the internal quantum-state distribution of the reactant to be controlled simultaneously and offers new applications in molecular science.

Acknowledgment. This work was supported by the National Natural Science Foundation of China under Grant Nos. 20603001, 10534010, 10634020, and 10821062 and the National Basic Research Program of China under Grant No. 2006CB806007.

References and Notes

(1) Yamanouchi, K. *Science* **2002**, *295*, 1659.
(2) Corkum, P. B.; Ellert, C.; Mehendale, M.; Dietrich, P.; Hankin, S.; Aseyev, S.; Rayner, D.; Villeneuve, D. *Faraday Discuss.* **1999**, *113*, 47.
(3) Stapelfeldt, H.; Seideman, T. *Rev. Mod. Phys.* **2003**, *75*, 543.
(4) Friedrich, B; Herschbach, D. *Phys. Rev. Lett.* **1995**, *74*, 4623.
(5) Seideman, T. *J. Chem. Phys.* **2001**, *115*, 5965.
(6) Kumar, G. R.; Gross, P.; Safvan, C. P.; Rajgara, F. A.; Mathur, D. *Phys. Rev. A* **1996**, *53*, 3098.
(7) Ortigoso, J.; Rodrıguez, M. *J. Chem. Phys.* **1999**, *110*, 3870.
(8) Seideman, T. *Phys. Rev. Lett.* **1999**, *83*, 4971.
(9) Machholm, M.; Henriksen, N. E. *Phys. Rev. Lett.* **2001**, *87*, 193001.
(10) Leibscher, M.; Averbukh, I. S.; Rozmej, P.; Arvieu, R. *Phys. Rev. A* **2004**, *69*, 032102.
(11) Rosca-Pruna, F.; Vrakking, M. J. J. *Phys. Rev. Lett.* **2001**, *87*, 153902.
(12) Hamilton, E.; Seideman, T.; Ejdrup, T.; Poulsen, M. D.; Bisgaard, C. Z.; Viftrup, S. S.; Stapelfeldt, H. *Phys. Rev. A* **2005**, *72*, 043402.
(13) Xu, N.; Wu, C.; Huang, J; Wu, Z.; Liang, Q.; Yang, H.; Gong, Q. *Opt. Express* **2006**, *14*, 4992.
(14) Kanai, T.; Minemoto, S.; Sakai, H. *Nature* **2005**, *435*, 470.
(15) Pavicic, D.; Lee, K. F.; Rayner, D. M.; Corkum, P. B.; Villeneuve, D. M. *Phys. Rev. Lett.* **2007**, *98*, 243001.
(16) Bartels, R. A.; Weinacht, T. C.; Wagner, N.; Baertschy, M.; Greene, C. H.; Murnane, M. M.; Kapteyn, H. C. *Phys. Rev. Lett.* **2002**, *88*, 013903.
(17) Shapiro, E. A.; Khavkine, I.; Spanner, M.; Ivanov, M. Y. *Phys. Rev. A* **2003**, *67*, 013406.
(18) Fleischer, S.; Averbukh, I. S.; Prior, Y. *Phys. Rev. A* **2006**, *74*, 041403(R). Fleischer, S.; Averbukh, I. S.; Prior, Y. *J. Phys. B* **2008**, *41*, 074018.
(19) Itatani, J.; Levesque, J.; Zeidler, D.; Niikura, H.; Pepin, H.; Kieffer, J. C.; Corkum, P. B.; Villeneuve, D. M. *Nature* **2004**, *432*, 867.
(20) Larsen, J. J.; Sakai, H.; Safvan, C. P.; Larsen, I. W.; Stapelfeldt, H. *J. Chem. Phys.* **1999**, *111*, 7774.
(21) Litvinyuk, I. V.; Lee, K. F.; Dooley, P. W.; Rayner, D. M.; Villeneuve, D. M.; Corkum, P. B. *Phys. Rev. Lett.* **2003**, *90*, 233003.
(22) Dooley, P. W.; Litvinyuk, I. V.; Lee, K. F.; Rayner, D. M.; Spanner, M.; Villeneuve, D. M.; Corkum, P. B. *Phys. Rev. A* **2003**, *68*, 023406.
(23) Lavorel, B.; Faucher, O.; Morgen, M.; Chaux, R. *J. Raman Spectrosc.* **2000**, *31*, 77.
(24) Renard, V.; Renard, M.; Rouzée, A.; Guérin, S.; H. Jauslin, R.; Lavorel, B.; Faucher, O. *Phys. Rev. A* **2004**, *70*, 033420.
(25) Renard, V.; Faucher, O.; Lavorel, B. *Opt. Lett.* **2005**, *30*, 70.
(26) Zamith, S.; Ansari, Z.; Lepine, F.; Vrakking, M. J. J. *Opt. Lett.* **2005**, *30*, 2326.
(27) Holmegaard, L.; Viftrup, S. S.; Kumarappan, V.; Bisgaard, C. Z.; Stapelfeldt, H. *Phys. Rev. A* **2007**, *75*, 051403(R).
(28) Renard, M.; Hertz, E.; Lavorel, B.; Faucher, O. *Phys. Rev. A* **2004**, *69*, 043401.
(29) Horn, C.; Wollenhaupt, M.; Krug, M.; Baumert, T. *Phys. Rev. A* **2006**, *73*, 031401(R).
(30) Hertz, E.; Rouzée, A.; Guérin, S.; Lavorel, B.; Faucher, O. *Phys. Rev. A* **2007**, *75*, 031403(R).
(31) Rouzee, A.; Hertz, E.; Lavorel, B.; Faucher, O. *J. Phys. B: At., Mol. Opt. Phys.* **2008**, *41*, 074002.
(32) Renard, M.; Hertz, E.; Guérin, S.; Jauslin, H. R.; Lavorel, B.; Faucher, O. *Phys. Rev. A* **2005**, *72*, 025401.
(33) Ghafur, O.; Rouzee, A.; Gijsbertsen, A.; Siu, W. K.; Stole, S.; Vrakking, M. J. J. *Nat. Phys.* **2009**, *5*, 289.
(34) Leibscher, M.; Averbukh, I. S.; Rabitz, H. *Phys. Rev. A* **2004**, *69*, 013402.
(35) Averbukh, I. S.; Arvieu, R. *Phys. Rev. Lett.* **2001**, *87*, 163601.
(36) Bisgaard, C. Z.; Viftrup, S. S.; Stapelfeldt, H. *Phys. Rev. A* **2006**, *73*, 053410.
(37) Bisgaard, C. Z.; Poulsen, M. D.; Peronne, E.; Viftrup, S. S.; Stapelfeldt, H. *Phys. Rev. Lett.* **2004**, *92*, 173004.
(38) Lee, K. F.; Litvinyuk, I. V.; Dooley, P. W.; Spanner, M.; Villeneuve, D. M.; Corkum, P. B. *J. Phys. B* **2004**, *37*, L43.
(39) Lee, K. F.; Shapiro, E. A.; Villeneuve, D. M.; Corkum, P. B. *Phys. Rev. A* **2006**, *73*, 033403.
(40) Hertz, E.; Faucher, O.; Lavorel, B.; Chaux, R. *J. Chem. Phys.* **2000**, *113*, 6132.
(41) Li, Y.; Liu, P.; Zhao, S.; Zeng, Z.; Li, R.; Xu, Z. *Chem. Phys. Lett.* **2009**, *475*, 183.
(42) Zeng, G.; Wu, C.; Jiang, H.; Gao, Y.; Xu, N.; Gong, Q. *J. Phys. B* **2009**, *42*, 165508.
(43) Fleischer, S.; Averbukh, I. S.; Prior, Y. *Phys. Rev. Lett.* **2007**, *99*, 093002.

(44) Gao, Y.; Wu, C.; Xu, N.; Zeng, G.; Yang, H.; Gong, Q. *Phys. Rev. A* **2008**, *77*, 043404.

(45) Lee, K. F.; Villeneuve, D. M.; Corkum, P. B.; Shapiro, E. A. *Phys. Rev. Lett.* **2004**, *93*, 233601.

(46) Underwood, J. G.; Sussman, B. J.; Stolow, A. *Phys. Rev. Lett.* **2005**, *94*, 143002.

(47) Lee, K. F.; Villeneuve, D. M.; Corkum, P. B.; Stolow, A.; Underwood, J. G. *Phys. Rev. Lett.* **2006**, *97*, 173001.

(48) Viftrup, S. S.; Kumarappan, V.; Trippel, S.; Stapelfeldt, H. *Phys. Rev. Lett.* **2007**, *99*, 143602.

(49) Wu, C.; Zeng, G.; Gao, Y.; Xu, N.; Peng, L.-Y.; Jiang, H.; Gong, Q. *J. Chem. Phys.* **2009**, *130*, 231102.

(50) Press, W. H.; Flannery, B. P.; Teukolsky, S. A.; Vetterling, W. T. *Numerical Recipes*, 2nd ed.; Cambridge University Press: Cambridge, 1992.

(51) Leibscher, M.; Averbukh, I. S.; Rabitz, H. *Phys. Rev. Lett.* **2003**, *90*, 213001.

(52) Torres, R.; Nalda, R. D.; Marangos, J. P. *Phys. Rev. A* **2005**, *72*, 023420.

(53) Xu, N.; Wu, C.; Gao, Y.; Jiang, H.; Yang, H.; Gong, Q. *J. Phys. Chem. A* **2008**, *112*, 612.

(54) Meijer, A. S.; Zhang, Y.; Parker, D. H.; Zande, W. J. *Phys. Rev. A* **2007**, *76*, 023411.

(55) Mouritzen, A. S.; Molmer, K. *J. Chem. Phys.* **2006**, *124*, 244311.

(56) Rakitzis, T. P.; Van den Brom, A. J.; Janssen, M. H. M. *Science* **2004**, *303*, 1852.

(57) Hasegawa, H.; Ohshima, Y. *Phys. Rev. A* **2006**, *74*, 061401(R).

(58) Holmegaard, L.; Nielsen, J. H.; Nevo, I.; Stapelfeldt, H. *Phys. Rev. Lett.* **2009**, *102*, 023001.

(59) Kong, W. *Int J. Mod. Phys. B* **2001**, *15*, 3471.

JP905743V